Polymer Chemistry

PAPER

View Article Online
View Journal | View Issue

CrossMark click for updates

Cite this: *Polym. Chem.*, 2016, **7**, 1756

Using Hansen solubility parameters to predict the dispersion of nano-particles in polymeric films

S. Gårdebjer,*[a,b] M. Andersson,[c] J. Engström,[d] P. Restorp,[d] M. Persson[b,d] and A. Larsson[a,b]

Received 4th December 2015,
Accepted 20th January 2016

DOI: 10.1039/c5py01935d

www.rsc.org/polymers

We suggest a rough and straightforward method to predict the dispersibility of modified cellulose nanocrystals (CNC) in nanocomposites using Hansen solubility parameters (HSP). The surface of CNC was modified using a novel approach where Y-shaped substituents with two different carbon chain lengths were attached to the surface. Approximate HSP values were calculated for the modified CNC, and dispersions of unmodified and modified CNC in solvents with varying HSPs were studied. The best dispersibility was observed in dichloromethane, when the CNC surface was modified with longer carbon chains. Dichloromethane has HSP similar to low-density polyethylene (LDPE). Nanocomposites with both unmodified and modified CNC were produced. The materials with modified CNC showed increased adhesion between the filler and the matrix, followed by a decreased water permeability compared to unmodified CNC, suggesting a better dispersibility of modified CNC in LDPE and confirming the usefulness of this approach.

Introduction

Incorporation of nano-rods to enhance the mechanical and barrier properties of a thermoplastic polymer has been widely studied.[1–4] One type of nano-rods that can be used is cellulose nanocrystals (CNC) which are derived from natural cellulose sources. CNC have high strength and stiffness and are usually produced *via* acid hydrolysis.[5,6] A major problem with the production of these nanocomposites, where a hydrophobic matrix material is combined with the more hydrophilic cellulose, is that the CNC tend to form aggregates, which results in inhomogeneous nanocomposite films.[5,7,8] By attaching hydrophobic chains to the surface of cellulose, the CNC become more similar to the matrix material; hence, an increased compatibility between the matrix and the filler can be achieved.[1,9,10] The cellulose surface modification can be done by polymerizing hydrophobic chains directly on the surface, for example, using a ring opening polymerization.[10–13] It is often difficult to determine the length of the final chains attached to the surface and several complementary analysis techniques need to be used. Another way to modify the surface of cellulose is to simply attach a known reactant to the surface; in this way the chemical structure of the substituent will be directly known.[1,14] In a recent study, CNC were chemically modified with substituents of either 6, 12 or 18 carbon atoms in a straight chain and nanocomposites of LDPE were produced.[1] An increased homogeneity and dispersion was observed when longer chains were attached to the surface. In this study, we use a similar approach with varying chain lengths but we use a Y-shaped substituent and attach it to the surface of CNC as shown in Fig. 1.

Even though there is a large amount of published work on different types of surface modifications, it can be difficult to predict the behavior and dispersibility of newly modified CNC in a matrix. Hansen and Hildebrand solubility parameters can be used to predict the solubility of polymers in different solvents.[15] Similar methods for predicting the dispersibility of CNC as fillers in nanocomposites are available, however the

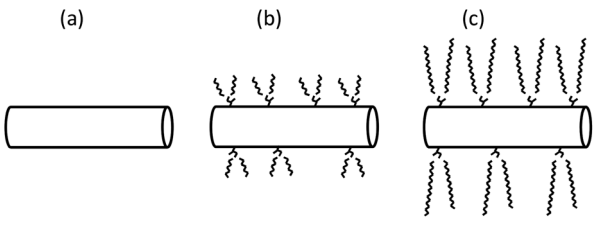

Fig. 1 Schematic image of the surface modification of CNC (a), where two types of chlorohydrins were used as reagents, one with chains consisting of 6 carbons as shown in (b) and one with chains consisting of an average of 17 carbons as shown in (c).

[a]*Department of Chemistry and Chemical Engineering, Chalmers University of Technology, 412 96 Göteborg, Sweden. E-mail: sofie.gardebjer@chalmers.se*
[b]*SuMo Biomaterials, VINN Excellence Centre, Chalmers University of Technology, 412 96 Göteborg, Sweden*
[c]*SP Technical Research Institute of Sweden, Box 5607, 114 86, Sweden*
[d]*AkzoNobel Pulp and Performance Chemicals AB, 445 80 Bohus, Sweden*

theoretical derivations of these methods give limited support that one could use them to predict the dispersion of CNC in solvents or polymer matrix materials. Recently, the dispersibility of single-walled carbon nanotubes has been measured in a large amount of solvents with varying Hildebrand and Hansen solubility parameters to propose appropriate solubility parameters for the nanotubes and graphene.[16] In another study, the Hildebrand solubility parameter for boron nitride nanotubes was extracted from light scattering experiments.[17] To achieve good properties of nanocomposites it is essential that the filler materials are well dispersed in the matrix. For established filler materials, the industry has experience on how to disperse the fillers and obtain good nanocomposites, but for new modified fillers we urgently need calculation methods to rationalize and predict whether successful nanocomposites can be manufactured or not. In this study, we suggest a rough method using the standard calculation tool for Hansen solubility parameters for polymers and apply it to surface modified CNC when knowing the chemical structure of the substituents and approximately the degree of surface coverage.

The aim of this study was two-fold: first to introduce a new way of modifying CNC by attaching Y-shaped hydrophobic chains to the surface of CNC by the reaction of a chlorohydrin. Second, we suggest a new efficient way of predicting the compatibility between modified CNC and a matrix material of low density polyethylene (LDPE). Our hypothesis was that the dispersion behavior of CNC in solvents with different Hildebrand and Hansen solubility parameters will mirror the dispersibility of the nanocomposites in matrix polymers. Furthermore, we assume that the Hansen solubility parameters could be predicted for surface modified CNC by using a computer method developed for compatibility studies of polymers in different solvents. Additionally, we also incorporate the unmodified and modified CNC in a matrix of LDPE, and show that our hypothesis seems to be valid. To support our work an extensive characterization of the nanocomposites was made.

Theoretical background

This section aims to describe the thermodynamics of a system of the solvent and/or polymer in combination with nano-rods. In order to mix two materials, thermodynamics require that Gibbs free energy, ΔG_{mix}, is zero or smaller at a certain temperature given by

$$\Delta G_{mix} = \Delta H_{mix} - T\Delta S_{mix} < 0 \quad (1)$$

where ΔH_{mix} is the enthalpy of mixing and ΔS_{mix} is the entropy of mixing. It should be noted that a negative sign on ΔG_{mix} could also be a result of phase-separation resulting in a stable structure and hence no mixing and/or dissolution. However, for the dissolution of polymers, the term ΔS_{mix} is positive due to the increased disorder. Flory has shown that ΔS_{mix} for a rigid rod, such as cellulose nanocrystals, can be described by assuming the formation of an isotropic solution at low concentration, and a nematic phase at higher concentrations according to eqn (2):[18,19]

$$\Delta S_{mix} = -\frac{k}{\nu_0}\left[(1-\phi)\ln(1-\phi) + \frac{\phi}{\frac{\nu_{NT}}{\nu_0}}\left(\ln\left(\frac{\phi}{x}\right) + (x-1)\right)\right] \quad (2)$$

where ΔS_{mix} is the entropy of mixing per volume of mixture, ϕ is the solute volume fraction, ν_0 and ν_{NT} are the solvent and rod molecular volume respectively and x is the aspect ratio of the rods. Since rigid rods are much larger than a polymer, nano-rods have relatively small ΔS_{mix} compared to polymers.[18]

For mixing of small molecules in a solvent, ΔH_{mix} can be expressed as the Flory–Huggins expression:[20]

$$\Delta H_{mix} = \chi\phi_1\phi_2 kT/\nu_0 \quad (3)$$

or as the Hildebrand–Scratchard expression:

$$\Delta H_{mix} = (\delta_{T,A} - \delta_{T,B})^2\phi_1\phi_2 \quad (4)$$

where χ is the Flory–Huggins interaction parameter, and $\delta_{T,A}$ and $\delta_{T,B}$ are the Hildebrand solubility parameters of the solute and the solvent. The Hildebrand solubility parameter was first described by Hildebrand and Scott and is defined as the square root of the cohesive energy density[21] according to eqn (5):

$$\delta_T = \sqrt{\frac{E_{coh}}{V}} \quad (5)$$

where V is the molar volume of the solvent and E_{coh} is the energy of vaporization. Combining eqn (3) and (4) gives eqn (6):

$$\chi = \frac{\nu_0}{kT}(\delta_{T,A} - \delta_{T,B})^2 \quad (6)$$

where it can be seen that the Flory–Huggins parameter χ is always positive. Thereby, if mixing should occur, the solubility parameters for species A and B should be as close as possible in order to decrease χ and also ΔH_{mix} and ΔG_{mix}. It can be seen from eqn (4) that the concept using solubility parameters can never give negative ΔH_{mix}, which could happen for systems with specific interactions (*e.g.* hydrogen bonds). This is thus a limitation in the use of Hildebrand solubility parameters, and it is questionable to use this concept for such systems. In this study, the surface of CNC was modified with carbon chains and incorporated in LDPE, and no specific interactions are likely to occur. Even though the Hildebrand solubility parameters are well documented for many solvents,[22] it is also well known that it cannot describe a system alone. The Hildebrand parameter is based on geometric mean approximation which can only be used for molecules or compounds that interact through London or dispersion interactions. However, molecular interactions also depend on dispersive, polar and hydrogen bonding interactions, which are described by the Hansen solubility parameter. Using Hansen solubility parameters, the solubility is divided into three parts:

$$\delta_{TOT}{}^2 = \delta_D{}^2 + \delta_p{}^2 + \delta_H{}^2 \quad (7)$$

where δ_D, δ_P and δ_H represent the dispersion, polar and hydrogen-bonding interactions respectively.

Each component is evaluated indirectly and materials having similar Hansen solubility parameters have high affinity for each other.[23] Hansen solubility parameters for an unknown solvent or solute can be calculated by using software like Hansen Solubility Parameters in Practice (HSPiP).[24] The HSPiP software consists of a database of Hansen parameters for a large number of solvents, but also allows estimation of Hansen parameters using a molecular structure (entered in SMILES or InChI format) as the input. The obtained Hansen parameters are calculated by an adapted neural network methodology where the full Hansen database dataset has been fitted to a model which takes inter-group interactions into account. Skaarup and Hansen further developed an equation to calculate the solubility parameter distance, R, between two materials:[23]

$$R = \sqrt{4(\delta_{D,1} - \delta_{D,2})^2 + (\delta_{P,1} - \delta_{P,2})^2 + (\delta_{H,1} - \delta_{H,2})^2} \quad (8)$$

These equations have so far been applied to low molecular weight molecules or polymers. In our case, we have nano-rods – which are aggregates of polymer chains and not single chains dispersed in a solvent as was the principal concept behind the models by Hansen and Skaarup. However, in comparison with the study of the dispersion of carbon nanotubes in solvents, we suggest that the Hansen parameters for the CNC should match the Hansen parameters for the solvents, where longer carbon chains on the surface give better dispersion of the nano-rods in the solvents. In order to make a first attempt following this suggestion, the unmodified and modified CNC will be dispersed in different solvents and the best dispersion in the solvent with similar Hansen solubility parameters to the matrix is suggested to give the best nanocomposite. This goes back to the Hildebrand discussion about cohesive energies around the solute and the solvent, assuming that the solvent only interacts with the surface of the solute (in this case the nano-rods). This means that the majority of the nano-rods have no influence on the dispersion neither in a solvent or matrix material. We also suggest that the software for the prediction of dispersibility in solvents for polymers could be used to calculate the Hansen parameter for a cellulose unit with either one or two substituents attached to the surface.

More in detail, it has been discussed for nano-rods whether the surface energy may be a more appropriate way to predict the dispersibility, instead of the cohesive energy. Bergin and coworkers suggested an equation:[18]

$$\chi_s = \frac{2v_0}{rkT}(\delta_{T,NT} - \delta_{T,sol})^2 \quad (9)$$

where r is the radius of a nano-rod and $\delta = \sqrt{E_{sur}}$ and E_{sur} are the surface energy of the nano-tubes and the solvent respectively. An interesting observation is that in eqn (9) the radius – and not the aspect ratio – is included. In an attempt to calculate $\delta_{T,NT}$, Bergin and co-workers used eqn (5) and incorporated expressions for the volume of the nano-rods and the surface energy required to detach the rods from each other in the dry state. By doing so, they could correlate to the surface energy rather than the cohesive energy according to:

$$\delta_T = 2\sqrt{\frac{E_{S,T}}{d}} \quad (10)$$

where E_{ST} is the surface energy and d is the diameter of the nano-rod. Eqn (9) suggests that the dispersion of nano-rods in a solvent (or polymer) is maximized when the surface energies are as equal as possible. The surface energy can also be affected by the attachment of carbon chains. Both the length of the chains and the surface coverage will have an impact on the surface energy. In eqn (10), δ_T correlates directly with the surface energies and one can assume that the same reasoning can be made for the dispersion of nano-rods in polymer matrices in composite materials.

Experimental

Production and surface modification of CNC

CNC were produced as described earlier by Bondeson *et al.*[25] In short, 40 g microcrystalline cellulose was hydrolyzed in 64% sulfuric acid for 130 minutes in 45 °C, followed by centrifugation at 4700 rpm (Sigma 4K15, Sigma Zentrifuges, Germany). The sediment was washed with several liters of deionized water and dialyzed in deionized water for 10 days, followed by ultrasonic treatment for 30 minutes on an ice bath. The CNC suspension was neutralized by the addition of 0.02 M NaOH and had a final concentration of approximately 0.5 wt%, and the reaction yield was 40%.

Fig. 1 shows a schematic image of the unmodified and modified CNC where Y-shaped chlorohydrin has been attached to the surface. The R-groups represent carbon chains of either 6 or an average of 17 carbons. The reaction was carried out in a 90 : 10 volume mixture of DMSO : toluene. Exchange of water was performed by adding DMSO to the water suspension of CNC, followed by evaporation of water in a rotary evaporator. An additional amount of toluene was added and the remaining water was evaporated by azeotrope formation with toluene.

The chemical modification of CNC was performed in a sealed round-bottomed reaction flask which contained 50 mL of a CNC-DMSO : toluene suspension and either C6 or C17 chlorohydrin; four equivalents were used to make sure to cover all the available sulfate ester groups on the CNC surface. The content of hydroxyl groups/sulfate ester groups available to react in the surface of CNC is approximately equal to 1.14×10^{-3} mmol OH^-,[26] meaning that 0.7 g and 1.2 g of chlorohydrins C6 and C17 were added, respectively. The reaction was carried out for 17 hours at 90 °C in an oil bath under constant mechanical stirring. The excess chlorohydrin was removed by adding the reaction mixture dropwise to a beaker with approximately 400 ml ethanol under constant stirring. The suspension was centrifuged at 5100 rpm for 10 minutes and the centrifugation was repeated twice. The washed modified CNC were kept in ethanol until further use. The modified CNC with the

different chlorohydrins are denoted as CNC6 and CNC17, respectively.

Characterization of modified CNC. Fourier Transform Infrared (FT-IR) analysis was performed on modified CNC, unmodified CNC and the pure chlorohydrins. The samples were pulverized and mixed with KBr at a ratio of 10 : 1 (KBr/sample). KBr-tablets with an area of 132 mm^2 were prepared by pressing the mixture at 1 ton for 1 min and then at 10 ton for 1 min. Spectra were scanned from 400 to 4000 cm^{-1} in a 2000 FT-IR spectrometer (Perkin-Elmer, England) with a resolution of 4.0 cm^{-1} and 20 scans per sample. A pure KBr-tablet was used for the background subtraction.

Elemental analysis (Vario Micro Cube, Frankfurt) was used to determine the amounts of carbon, nitrogen and oxygen in unmodified CNC as well as modified CNC. The sample was wrapped in small tin capsules and tin canisters and introduced into a firing tube where it was burned at 1150 °C. The product gases N_2, CO_2, H_2O and SO_2 were measured by using a hot wire detector.

Approximate Hansen solubility parameters for the addition of either one or two substituents to one glucose unit (Fig. 2) were calculated using the software Hansen Solubility in Practice (HSPiP) developed by Abbott and Yamamoto.[24] The reason why both one and two substituents were calculated is that it is not possible to know exactly how many substituents are attached per glucose, but using HSP values for both one and two substituents will give enough information to test the suggested hypothesis.

Dispersion test of cellulose nanocrystals in solvents with varying solubility parameters. Solvents with varying Hildebrand and Hansen solubility parameters were chosen according to Table 1. 0.5 wt% of the unmodified and modified CNC were added to the different solvents. Due to the large differences in solubility parameters, it is not possible to change directly from water to dichloromethane and the solvents with lower solubility parameters. Therefore, the solvent had to be exchanged by centrifugation, using either methanol or acetone as an intermediate solvent. In these cases the CNC were washed at least three times to remove all excess water and thereafter the desired solvent was added. The dispersibility of CNC in the different solvents was visually studied immediately after exchange.

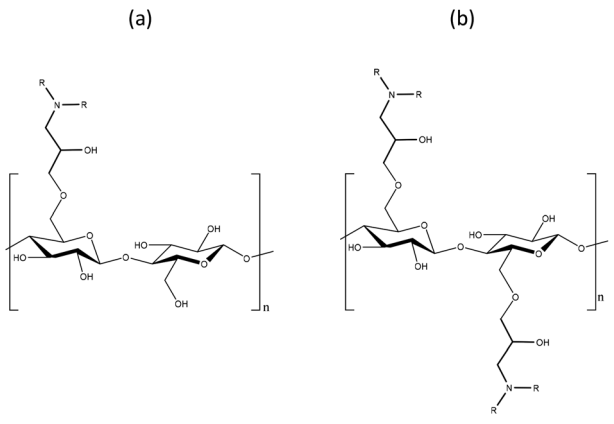

Fig. 2 Schematic image of the molecules used for the calculation of Hansen solubility parameters, in (a) one substituent and (b) two substituents. R represents carbon chains consisting of either 6 or an average of 17 carbons.

Table 1 Hildebrand (δ) and Hansen (δ_{TOT}) solubility parameters for the solvents used in the study[22] (where δ_D is the dispersive, δ_P is the polar and δ_H is the hydrogen bonding interactions of HSP)

Solvent	δ ($MPa^{1/2}$)	δ_{TOT} ($MPa^{1/2}$)	δ_D ($MPa^{1/2}$)	δ_P ($MPa^{1/2}$)	δ_H ($MPa^{1/2}$)
Water	23.5	47.8	15.6	16.0	42.3
Methanol	14.3	29.6	15.1	12.3	22.3
Ethanol	12.9	26.5	15.8	8.8	19.4
Butanol	11.3	23.2	16.0	5.7	15.8
Dichloromethane	9.8	20.2	18.2	6.3	6.1
Toluene	8.9	18.2	18.0	1.4	2.0
Heptane	7.4	15.3	15.3	0	0
LDPE[a]	7.9	17.8	16.5	5.9	4.1

[a] Ref. 27 and 28.

The parameters for LDPE are shown at the bottom of the table, where the Hildebrand parameter for LDPE is equal to 7.9 and the Hansen parameter is equal to 17.8 for LDPE.[27,28] Toluene and heptane have Hildebrand values closest to LDPE, while dichloromethane has similar Hansen solubility parameters. These solvents are therefore the preferred solvents to study for the indication of dispersibility of modified CNC in LDPE.

Production and characterization of nanocomposite materials

Nanocomposites were prepared by combining LDPE (Sigma Aldrich, USA) with either unmodified or modified CNC. The film preparation was done *via* solvent casting followed by hot-melt pressing. The filler contents were chosen to 1, 3, and 5 wt% to a total amount of 400 mg. The solvent of CNC or modified CNC was exchanged by centrifugation to *p*-xylene through several centrifugation steps using ethanol and dichloromethane as intermediate solvents. The dispersion of the different CNC and *p*-xylene was transferred to a glass vial and LDPE was added. The vial was placed in an oil bath with a temperature of 110 °C and left for LDPE to dissolve while stirred. The hot dispersion was immediately poured onto a pre-heated Petri dish (100 °C) and a lid was placed on top. The dishes were left in a fume hood to evaporate for 24 hours and the dry films were kept in a vacuum oven at 40 °C for three days. Nanocomposite films were hot-melt pressed at 120 °C and 3 bars for 4 minutes and the final films were kept in a desiccator with silica orange until use.

Film transparency was determined by measuring the percent transmittance between 1000 and 200 nm using a spectrophotometer (Agilent Technologies Cary60 UV-Vis, USA). Creep and strain recovery of the films were tested in a dynamic mechanical analyzer at 25 °C (DMA Q-800, TA Instruments, USA). Film samples of 5.7 mm width were mounted using a conventional film clamp. The average thickness of the films was 50 μm and the preload force was set to 0.01 N. The films

were displaced at a pressure of 1 MPa for 10 minutes and recovered for 10 minutes.

Permeability measurements were performed in diffusion cells.[8,29] A film sample, with recorded average thickness, was placed in between a donor and an acceptor chamber. 15 ml of MilliQ water was added to each chamber and 10 μl of ^{3}[H]-labeled water was added to the donor chamber. The solution was stirred by placing the diffusion chambers on a rotating table at 50 rpm (Edmund Bühler 7400, Germany). Due to the large difference in radioactivity between the donor and the acceptor chambers, the donor chamber concentration was considered to be constant during the whole experiment. Following the permeation measurement, samples of 500 μl were taken from the acceptor chamber and immediately replaced with an equal amount of pure MilliQ water. Samples were assayed with a scintillation liquid, Ultima Gold, and run on a liquid scintillation analyzer (Tri-Carb B2810TR, Perkin-Elmer, USA). The mass transfer rate was calculated according to eqn (11) using Fick's first law for the steady state mass transfer rate through a film:

$$J = DKA\frac{c_d - c_a}{h} = PA\frac{c_d - c_a}{h} \quad (11)$$

where J is the flux, c_d and c_a correspond to the donor and acceptor chamber concentrations respectively, A is the membrane area, h is the film thickness, D is the diffusion coefficient, K is the partition coefficient and P is the permeability. The flux J was calculated from the linear slope in a plot of accumulated water against time.

Results and discussion

This section will first describe a new method for the synthesis and characterization of the modified CNC. Thereafter, we use the modified CNC to suggest how one can predict the dispersion in nanocomposite materials in polymer matrixes by (i) dispersing the different CNC in solvents and (ii) dispersing CNC and modified CNC in the model polymer matrix (in this case LDPE). An extensive characterization of the films will be presented in the end to support the findings.

Characterization of surface modification

Fig. 3 shows the FT-IR spectra for the unmodified CNC (black line), modified CNC17 (dashed line) and the pure chlorohydrin (dotted line). The spectrum of the modified CNC is similar to the spectrum with unmodified CNC; however the peaks appearing around 2922 cm^{-1}, corresponding to methylene groups, are different for the unmodified and modified CNC. For the chlorohydrin, a second peak appears at 2852 cm^{-1} and a third at 1446 cm^{-1} which correspond to the methyl groups present only in the chlorohydrin. These peaks are also present for the modified CNC, which indicates a successful modification. Additionally, CNC are produced *via* acid hydrolysis using sulfuric acid, and therefore it is believed that the surface of CNC is covered with C–O–SO_3 groups.[30] The

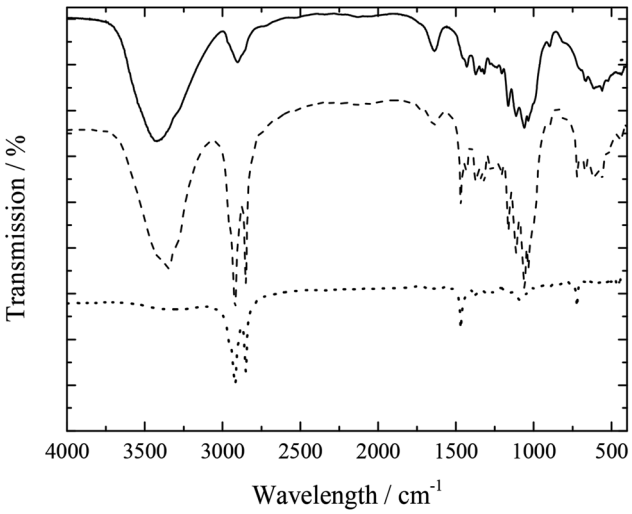

Fig. 3 FT-IR spectra of unmodified CNC (black line), the surface modified CNC17 (dashed line) and the pure chlorohydrin (dotted line) used in the reaction for surface modification.

peak at 807 cm^{-1} corresponds to the vibration of C–O–S and is present for both CNC and CNC17 which confirms the presence of sulfate ester groups.

Elemental analysis was performed on unmodified CNC and modified CNC and the amount of nitrogen was compared for the samples, since the chlorohydrins have nitrogen in the molecular structure. The unmodified CNC showed a nitrogen amount less than 0.2%, while CNC6 showed a value around 0.7%. CNC17 showed the highest value of nitrogen (1.4%), indicating that surface modification with the longest chains was most successful.

The average distance between substituents on the surface of nanocellulose was estimated to be around 5 Å for CNC17. This was done by using the nitrogen content and assuming that the size of the nano-rods are equal before and after substitution, and a density of the cellulose nano-rods equal to 1.5 g ml^{-1} and a diameter of 10 nm. This estimation shows that the coverage of substituents on the cellulose nanocrystals is high.

Dispersion of cellulose nanocrystals in solvents with varying solubility parameters

Hansen solubility parameters were calculated for the molecules presented in Fig. 2 as well as a cellulose unit without any substituents. Using eqn (8), the distance between the solvents and the unmodified and modified CNC could be calculated. Fig. 4a–c shows the calculated distances in the different solvents and photographs of the dispersions of unmodified and modified CNC going from higher to lower solubility parameters from left to right. According to the calculations, unmodified cellulose (Fig. 4a) has the shortest distance to methanol and hence should show the best dispersibility in this solvent, which can also be seen to be the case. However, water also shows an almost transparent appearance while the distance to water is equal to 22. It should be noted that the

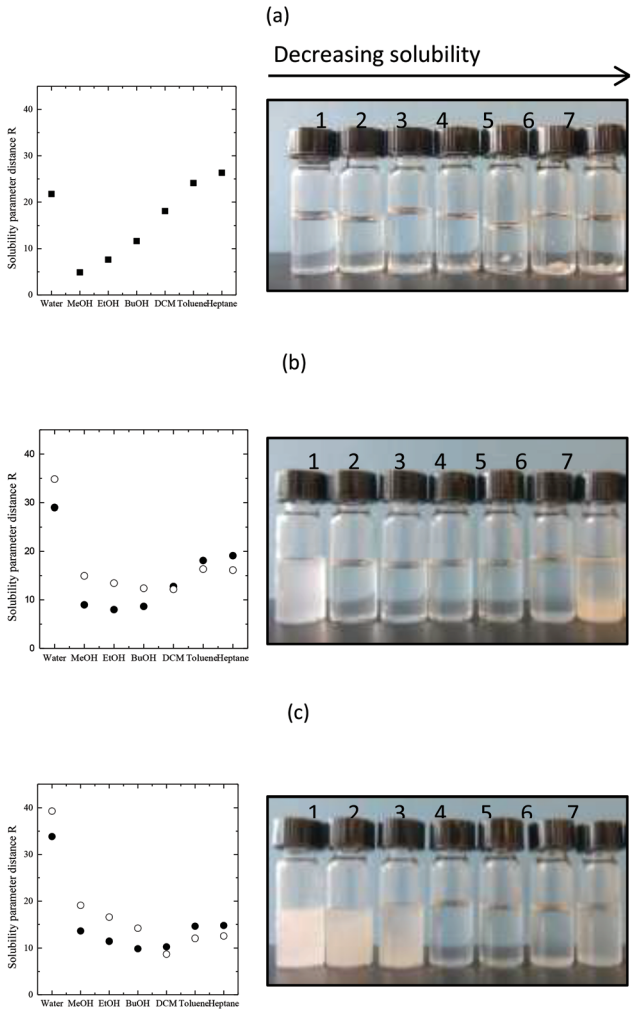

Fig. 4 Graphs showing calculated solubility parameter distances between the indicated solvents and unmodified cellulose (■), and cellulose with either one (○) or two (●) substituents attached. Photographs show the dispersion in the different solvents immediately after mixing in (a) unmodified CNC, (b) CNC6 and (c) CNC17.

CNC have charged sulfate ester groups attached on the surface, and are thereby stabilized by electrostatic interactions, which explains the good dispersion in water. Using solvents with lower solubility parameters resulted in aggregation of the unmodified cellulose, which can be seen as white assemblies in the bottom of the flask.

Fig. 4b shows the calculated distance for CNC modified with one or two attached substituents with short chains. In the graphs one can see that the calculated R values for one and two substituents vary as expected with the solubility parameters and have a minimum. This minimum appears different for one and two substituents, indicating as expected that the dispersibility of modified CNC in solvents depends on the number of attached substituents. For one substituent, MeOH, EtOH and BuOH show the shortest distances according to the graph. When instead two substituents were attached to the cellulose unit, BuOH and DCM are the preferred solvents. Studying the dispersions in the flasks, solvents 2–5 were observed to be the favored ones for the modified CNC6, while aggregation and sedimentation are seen for water, toluene and heptane, *i.e.* solvents 1, 6 and 7. Interestingly, the calculated R values for one and two substituents cross each other when the solubility parameters for the solvents are decreased. For the largest solubility parameters (water) the R values are lowest for CNC with two attached substituents per monomer unit compared to one unit and the opposite is observed for the solvent with the lowest solubility parameter. This appears at a first glance to be strange and can be explained by the differences in interaction parameters as presented in Fig. 5.

For the CNC17 with one chain attached to the cellulose unit, BuOH and DCM are the preferred solvents according to the graph (Fig. 4c). Two longer chains of C17 have the shortest distance to DCM according to eqn (8), which also correlates well with the observations in Fig. 4c. For the modified CNC17, solvents 1–3 show an opaque appearance, meaning that aggregation has occurred. Further, the dispersion looks more transparent in butanol, DCM and toluene, which indicates a better dispersion. However, solvent 8 *i.e.* heptane shows an opaque appearance and hence agglomeration has occurred.

Going into more detail, the different interaction parameters (δ_D, δ_P and δ_H) for the Hansen solubility parameters both for solvents and calculated ones for the CNC are shown in Fig. 5. Cellulose shows values closest to methanol while the addition of two substituents attached to the glucose units are closer to butanol and dichloromethane. It should also be noted that the longer chains show interaction parameters closer to dichloromethane compared to the shorter chains.

From these findings, it can be suggested that unmodified CNC have Hansen solubility parameters similar to methanol (δ_{TOT} = 29.6). The surface modification of CNC decreased the calculated Hansen solubility parameters for both CNC6 and CNC17 at the same time as clearer dispersions were observed for solvents correlating to values of δ_{TOT} = 23.2–29.6 for CNC6 and δ_{TOT} = 20.1–23.2 for CNC17. Since LDPE has the Hansen

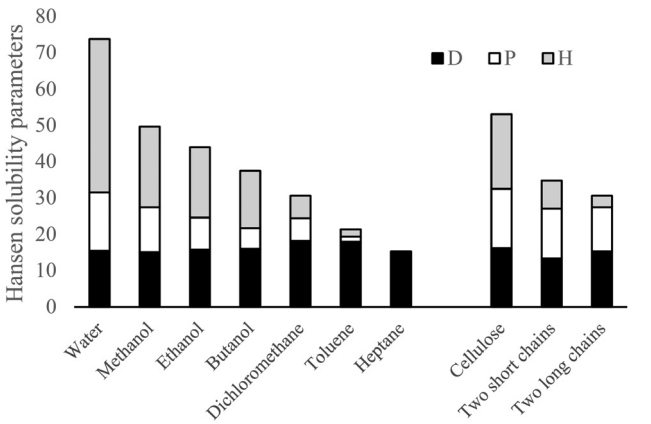

Fig. 5 Interaction parameters for Hansen solubility parameters. Tabulated values for the solvents used and the calculated values for cellulose and surface modified CNC are shown.

solubility parameters closest to DCM, this method suggests that the dispersion of CNC17 should be the most homogeneous, followed by CNC6 and unmodified CNC.

Characterization of nanocomposite materials

The transmittance, creep properties, and water permeability for the produced nanocomposites were studied. The films were produced by solvent casting from *p*-xylene, followed by hot-melt pressing. The appearance of the films after solvent casting was a bit opaque. This can be due to solvent residues or the formation of pores in the films during the casting as earlier discussed.[8] After hot-melt pressing, the films were more or less transparent and no major differences could be seen by visual inspection. The transmittance was measured using UV-Vis at 660 nm. Pure LDPE showed the highest transmittance of 95%. The addition of both unmodified and modified CNC resulted in a decreased transmittance, for unmodified CNC 66 ± 3% and for CNC6 65 ± 6%. The films with modified CNC17 showed the smallest decrease and a transmittance of 73 ± 4% were observed for these films. The smaller decrease indicates that the nano-rods with the longer chains attached to the surface are better dispersed in the matrix.

Fig. 6a and b shows the creep and strain recovery for pure LDPE as well as the films consisting of 5 wt% unmodified and modified CNC. The film of pure LDPE as well as the films containing unmodified CNC or CNC6 crept to approximately 130%, while the film with CNC17 only crept to 97%. Since the creep was not affected after the addition of unmodified CNC or CNC6, this indicates that the adhesion is poor between LDPE and unmodified CNC and between LDPE and CNC6. For the films with an addition of 5 wt% CNC17, an increased adhesion between the matrix and filler modified CNC can explain the improved resistance to creep. The film with CNC17 does also recover the fastest to an extent of 93%. The nanocomposite with CNC6 does also recover to 93% but takes a bit longer time. Pure LDPE films and the films with unmodified CNC recover to 90% and 89% respectively.

Water permeability was measured in diffusion cells and the results are shown in Fig. 7. Pure LDPE films showed a water permeability of 6.6×10^{-13} m^2 s^{-1} while the addition of unmodified CNC resulted in an increased water permeability compared to pure LDPE. However, the high standard deviations for the unmodified CNC make it difficult to interpret the data and are probably a result of the poor dispersion and aggregation in the hydrophobic matrix. The addition of modified CNC6 resulted in a small decrease of the water permeability compared with the pure LDPE film. The addition of CNC17 resulted in a larger decrease of water permeability compared to pure LDPE. According to Nielsen theory, the addition of an impermeable filler is believed to decrease the permeability due to an increased tortuosity path for the permeant.[31] Another factor known to decrease the permeability is increased crystallinity of the matrix, which can be induced upon the addition of a filler. In these cases, the filler functions as a nucleating site from where crystals can grow in the matrix material. This has been shown to be advantageous when the filler is well dispersed.[13] In our case, the addition of CNC17 is believed to result in improved dispersion compared to unmodified CNC and CNC6, which is strengthened by the results from the creep test. Another important issue is that even if the filler is considered impermeable, there could be available sites where water molecules could be trapped, hence resulting in a decreased water permeability when the water in that case follows the dual-sorption kinetics. Improved dispersibility is advantageous also in this case. If so, the permeability should be lowest for the nanocomposites where CNC17 has been added, which has been confirmed in Fig. 7.

In summary, we have presented a new method to synthesize the surface of cellulose nanocrystals and we have made a first trial to suggest a rough and straightforward method where we can predict good dispersibility in a hydrophobic polymer by the use of solvents with varying Hansen solubility parameters. The modified CNC with the longest chains attached to the surface dispersed well in LDPE, in agreement with the results from the dispersibility test in different solvents. The properties

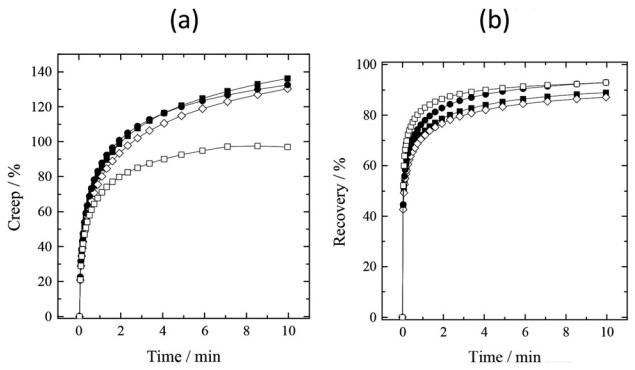

Fig. 6 (a) Creep and (b) strain recovery for the composite films consisting of 5 wt% CNC, showing LDPE (■), CNC (◊), CNC6 (●), and CNC17 (□) (n = 2).

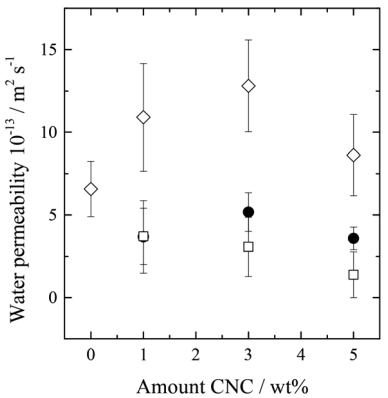

Fig. 7 Water permeability of LDPE and the composite films showing the addition of CNC (◊), CNC6 (●), and CNC17 (□) (n = 3–5).

such as creep resistance and strain recovery of the composite materials were improved compared to the pure LDPE films or the films with unmodified CNC. Water permeability decreased for the nanocomposites with modified CNC, which indicates an improved adhesion and compatibility between the filler and the matrix material. It should however be pointed out that it was only the dispersibility of three different nano-fillers that was tested in one polymer in this study. Other effects such as conformation entropy and steric constraints due to the surface modification could have an impact on the dispersibility and to further validate the suggested method several nano-fillers and polymers have to be evaluated. One way to do so is to disperse CNC in several solvents, and correlate the Hansen solubility parameters directly with different polymers.

Conclusions

This study proposes a simple and straightforward approach to predict the dispersion of unmodified and modified cellulose nanocrystals in a hydrophobic polymer. At the same time, we present a new method for the surface modification of cellulose with a Y-shaped substituent. Two different chain lengths of the substituent were used and approximate Hansen solubility parameters were calculated for modified and unmodified CNC. Longer chains on the substituent suggested improved dispersion in a hydrophobic polymer, which was shown when producing nanocomposite materials of LDPE. The creep and recovery properties as well as the water permeability of the produced composite materials were studied and the results showed that surface modification with longer chains improved the adhesion between the matrix and the filler. The water permeability also decreased to a higher extent for the materials with longer carbon chains on CNC, which can indicate a better adhesion between the filler and the matrix materials. However, in order to fully validate this suggested method, dispersion of the CNC should be tested in additional solvents. These solvents should then be chosen to correlate their Hansen solubility values with different polymers.

Acknowledgements

The financial support from VINN Excellence SuMo Biomaterials (Supramolecular Biomaterials – Structure dynamics and properties) is gratefully acknowledged. We would also like to acknowledge masters student Aina Viladot for help with experimental work and Elin Persson at AkzoNobel, Sweden for help with elemental analysis.

References

1 A. Junior de Menezes, G. Siqueira, A. A. S. Curvelo and A. Dufresne, *Polymer*, 2009, **50**, 4552–4563.
2 M. Hietala, A. P. Mathew and K. Oksman, *Eur. Polym. J.*, 2013, **49**, 950–956.
3 K. Hossain, I. Ahmed, A. Parsons, C. Scotchford, G. Walker, W. Thielemans and C. Rudd, *J. Mater. Sci.*, 2012, **47**, 2675–2686.
4 F. Hussain, M. Hojjati, M. Okamoto and R. E. Gorga, *J. Compos. Mater.*, 2006, **40**, 1511–1575.
5 M. A. S. Azizi Samir, F. Alloin and A. Dufresne, *Biomacromolecules*, 2005, **6**, 612–626.
6 D. Klemm, F. Kramer, S. Moritz, T. Lindström, M. Ankerfors, D. Gray and A. Dorris, *Angew. Chem., Int. Ed.*, 2011, **50**, 5438–5466.
7 A.-L. Goffin, J.-M. Raquez, E. Duquesne, G. Siqueira, Y. Habibi, A. Dufresne and P. Dubois, *Biomacromolecules*, 2011, **12**, 2456–2465.
8 S. Gårdebjer, A. Bergstrand and A. Larsson, *Eur. Polym. J.*, 2014, **57**, 160–168.
9 E. Espino-Pérez, J. Bras, V. Ducruet, A. Guinault, A. Dufresne and S. Domenek, *Eur. Polym. J.*, 2013, **49**, 3144–3154.
10 H. Lönnberg, Q. Zhou, H. Brumer, T. T. Teeri, E. Malmström and A. Hult, *Biomacromolecules*, 2006, **7**, 2178–2185.
11 H. R. Kricheldorf, *Chemosphere*, 2001, **43**, 49–54.
12 T. Endo, Y. Shibasaki and F. Sanda, *J. Polym. Sci., Part A: Polym. Chem.*, 2002, **40**, 2190–2198.
13 S. Gårdebjer, A. Bergstrand, A. Idström, C. Börstell, S. Naana, L. Nordstierna and A. Larsson, *Compos. Sci. Technol.*, 2015, **107**, 1–9.
14 N. Lin, J. Huang, P. R. Chang, J. Feng and J. Yu, *Carbohydr. Polym.*, 2011, **83**, 1834–1842.
15 A. Agrawal, A. D. Saran, S. S. Rath and A. Khanna, *Polymer*, 2004, **45**, 8603–8612.
16 S. D. Bergin, Z. Sun, D. Rickard, P. V. Streich, J. P. Hamilton and J. N. Coleman, *ACS Nano*, 2009, **3**, 2340–2350.
17 M. Mutz, E. Eastwood and M. D. Dadmun, *J. Phys. Chem. C*, 2013, **117**, 13230–13238.
18 S. D. Bergin, V. Nicolosi, P. V. Streich, S. Giordani, Z. Sun, A. H. Windle, P. Ryan, N. P. P. Niraj, Z.-T. T. Wang, L. Carpenter, W. J. Blau, J. J. Boland, J. P. Hamilton and J. N. Coleman, *Adv. Mater.*, 2008, **20**, 1876–1881.
19 P. J. Flory, *Principles of Polymer Chemistry*, Cornell University Press, Ithaca, NY, 1953.
20 M. Rubinstein and R. H. Colby, *Polymer Physics*, Oxford Univeristy Press, Oxford, 1st edn, 2003.
21 J. Hildebrand and R. L. Scott, *The solubility of nonelectrolytes*, Reinhold, New York, 1950.
22 J. Brandrup, E. H. Immergut, G. E. A. A. Akihiro and D. R. Bloch, *Polymer Handbook*, Wiley & Sons, New York, 4th edn, 1999.
23 C. M. Hansen and K. Skaarup, *J. Paint Technol.*, 1967, **39**, 511–514.
24 S. Abbott and H. Yamamoto, *Hansen Solubility in Practice*, http://hansen-solubility.com.

25 B. Bondeson, A. Mathew and K. Oksman, *Cellulose*, 2006, **13**, 171–180.
26 S. Eyley, S. Shariki, S. E. C. Dale, S. Bending, F. Marken and W. Thielemans, *Langmuir*, 2012, **28**, 6514–6519.
27 C. M. Hansen, *Hansen Solubility Parameters - A User's Handbook*, CRC Press, Boca Raton, FL, 2007.
28 D. W. van Krevelen and K. T. Nijenhuis, in *Properties of Polymers*, ed. D. W. van Krevelen and K. T. Nijenhuis, Elsevier, Amsterdam, 4th edn, 2009, pp. 189–227, DOI: 10.1016/B978-0-08-054819-7.00007-8.
29 H. Andersson, J. Hjärtstam, M. Stading, C. von Corswant and A. Larsson, *Eur. J. Pharm. Sci.*, 2013, **48**, 240–248.
30 M.-J. Wang, Y.-L. Xie, Q.-D. Zheng and S.-J. Yao, *Ind. Eng. Chem. Res.*, 2009, **48**, 5276–5284.
31 L. E. Nielsen, *J. Macromol. Sci., Part A: Chem.*, 1967, **1**, 929–942.